ACS OMEGA

http://pubs.acs.org/journal/acsodf

Article

Material Properties of Traditional Handmade Paper Samples Fabricated from Cellulosic Fiber of Lokta Bushes

Girja Mani Aryal, Krishna Prasad Kandel, Ram Kumar Bhattarai, Basant Giri, Menuka Adhikari, Alisha Ware, Shubo Han, Gibin George, Zhiping Luo, Bhoj Raj Gautam,* and Bhanu Bhakta Neupane*

Cite This: *ACS Omega* 2022, 7, 32717−32726

Read Online

ACCESS | Metrics & More | Article Recommendations | Supporting Information

ABSTRACT: Handmade papers (HPs) are fabricated from fibrous biomass of Lokta bushes and other plant species following traditional eco-friendly method in Nepal. Although HP fabricated from Lokta bushes is believed to be durable and resistant to bugs and molds, material properties of this paper are not reported in literature. In this study, we measured several material properties of 10 handmade Lokta paper samples collected from local enterprises and paper industries. The mean caliper, grammage, apparent density, equilibrium moisture content, Cobb 60, brightness, opacity, tensile strength, and tensile index values in the paper samples ranged from ∼90 to 700 μm, 50 to 150 g/m^2, 0.2 to 0.4 g/cm^3, 4 to 7%, 50 to 400 g/m^2, 56 to 67%, 83 to 98%, 30 to 2900 N/m, and 1 to 27 Nm/g, respectively. These properties suggested that the HPs are lightweight papers with intermediate to high strength. The tensile strength was found to be significantly higher along the length direction ($p < 0.05$). Characteristic features of cellulose, hemicellulose, and lignin were observed in FTIR spectra. The crystalline and amorphous phases were also identified in X-ray diffraction (XRD) data. Electron microscopy images revealed a nicely cross-linked network of intact fibers having almost parallel arrangement of microfibrils. These features could provide strength and durability to the paper samples. Understanding the material properties of HPs down to the sub-microscopic level may help improve the paper quality and find novel applications in the future.

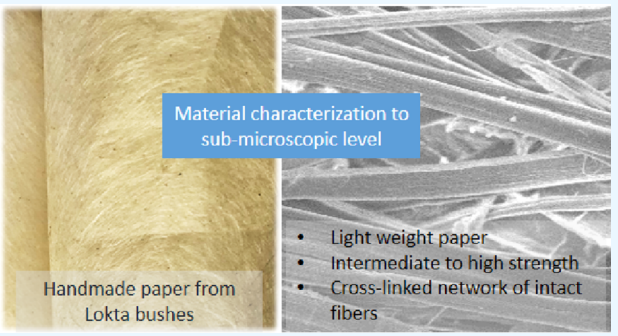

1. INTRODUCTION

Handmade paper (HP) making has been practiced across the globe since 105 AD.[1] It is believed that handmade paper making started, at least, in the 12th century AD in the western district of Baglung in Nepal.[2] In Nepal, HP is known as Nepali Kagaj. It is a traditional paper made from fibrous biomass of Lokta (*Daphne bholua* and *Daphne papyracea*) and Argeli (*Edgeworthia gardneri*) or their combinations. These plants are found at an elevation of 1600−4000 m in Nepal.[2−5] HP is believed to be a durable and bug- and mold-resistant paper and therefore is mostly used in official record keeping and religious texts.[3] Furthermore, a number of value-added products such as notebooks, photo albums, gift boxes and bags, and paper jewelries are fabricated from HP. The HP made from Lokta bushes is traditionally named Loka paper. However, any HP made from other plants is loosely termed as Lokta paper these days. There are ∼200 small- and medium-sized paper-making enterprises in Nepal, which support the livelihood of ∼55,000 families with an annual sell value of ∼$2.5 and ∼5.5 million in Nepal and abroad, respectively.[3]

HP making starts from harvesting stalks and manual removal of outer scaly bark. The long fiber mass is cut into small pieces and soaked in cold water for 6−12 h, and debris is removed manually. The biomass is boiled in water or ash solution for around 5−10 h. Next, the softened fiber biomass is beaten to make pulp and dispersed in water to make slurry. The slurry is poured in a wooden mesh frame or paper molds over a water tank, drained, and air-dried to obtain the paper sheet. In recent years, the hot water or ash solution digestion step of paper making is replaced by 4−5% hot alkali solution treatment for 3−10 h. Depending on the customers' need, additional steps such as chemical bleaching, calendaring, and machine glazing are performed.[3,4] The paper can be colored using traditional plant-based or commercial dyes if needed. Traditional HP making is considered an eco-friendly process since it requires low energy consumption, and little or no chemicals are used compared to the commercial paper-making process.

In recent years, several research groups are exploring the handmade paper making in laboratory settings. The paper sheets are fabricated from woody or non-woody parts of different plant species following mechanical and chemical methods of fiber

Received: July 12, 2022
Accepted: August 23, 2022
Published: September 1, 2022

https://doi.org/10.1021/acsomega.2c04398
ACS Omega 2022, 7, 32717−32726

processing or their combination.[6−11] A number of factors such as length and strength of individual fiber, organization of fiber, degree of cross-linking and bonding, chemical composition of fiber and processing parameters, extent of fibrillation, fines, and crill content determine the strength of a paper sheet.[12−18] The long fibers can form more contact points than short fibers, eventually leading to the paper of higher strength. However, the long fibers lead to the increased tendency to fiber entanglement and floc formation during processing.[14,19] The fiber aspect ratio, surface morphology, and chemical composition also affect the paper properties.[12] To understand the end properties of a paper sheet, it is particularly important to understand the material properties down to sub-microscopic levels.

Although HP fabricated from Lokta bushes is believed to be durable and resistant to bugs and molds, material properties of this paper are not reported in the literature. In this research, we determined the physical, optical, mechanical, and chemical properties of 10 HP samples collected from different paper enterprises of Nepal. A correlation between different parameters is provided, and the data are compared with other types of papers. We also compared the properties of paper sheet with raw Lokta fiber to understand the change in those properties during the paper-making process. Finally, we suggest few strategies to improve the HP quality and the potential applications of the HP Lokta paper.

2. MATERIALS AND METHODS

2.1. Materials. We collected 10 handmade Nepali paper samples, hereunder labeled from P1-10, from local paper enterprises directly. A total of 20 paper sheets (∼60 cm× 100 cm) made in the same lot were collected for each paper type. The samples were stored in an airtight container in dark until performing experiments.

Raw Lokta fiber was obtained from the fibrous inner bark of Lokta bushes collected from Baglung District of Nepal. The outer scaly bark was manually removed, and the fiber biomass was air-dried and then used for further study.

All the chemicals used in the study were purchased from Thermo Fisher Scientific India Pvt. Ltd and were used without further purification. All reagents were made in double-distilled water (pH = 7.1 ± 0.1 and conductivity 5 ± 1 μS).

2.2. Methods. *2.2.1. Measurement of Physical Properties.* We measured the thickness of a paper sheet (caliper) using a digital thickness micrometer (Hans Schmidt, D2000C) following the TAPPI T411 method.[20] Six independent measurements at different regions of the paper sheet were made.

Grammage or basic weight of the paper samples was measured following the TAPPI-410 method[21] under standard conditions of 23 °C temperature and 50% relative humidity (RH). Briefly, a paper sheet of 500 cm^2 was cut with a circular cutter, and its weight was taken (±0.001 g). Grammage (g/m^2) was obtained by taking the ratio of weight of paper (g) and its area (m^2). Six independent measurements were performed for each sample.

To measure the moisture content under ambient conditions, 2.000 g of the paper sample conditioned at 23 °C and 50% RH was placed in an oven (105 ± 2 °C) for 24 h. The sample was cooled in a non-hygroscopic desiccator and weighed. The difference in the weight before and after drying was used to calculate the moisture content of the paper. Three independent measurements were taken for each sample.

The Cobb 60 value was measured following the TAPPI-T441 method[22] for non-bibulous paper using a standard Cobb sizing tester. The excess water from the wetted specimen was removed by rolling a hand roller (10 kg) one back and one forward without applying additional pressure. The difference in weight of the paper after and before wetting was used to estimate the Cobb 60 value.

The opacity and brightness (ISO brightness) of the paper were determined using a standard brightness-opacity tester (UEC1018, India). Five paper specimens of size 5 mm × 5 mm were cut and put in the tester to determine the optical properties.

Tensile strength was determined under standard conditions of 23 °C and 50% RH using a tensile machine (UEC1005B, India) having a load capacity of 5−50 kg. Ten paper specimens of size 15 mm × 25 mm were cut for each paper. The cut piece was loaded in the tester to determine the strength along the length direction (LD) and cross direction (CD) of the wooden frame of paper molds. The tensile index (Nm/g) was calculated by dividing tensile strength of a paper (N/m) by its basic weight or grammage (g/m^2).

2.2.2. Determination of Chemical Composition. Lignin, cellulose, hemicellulose, and ash contents of the paper and fiber samples were determined gravimetrically following standard test methods.[23−26] To determine the cellulose content, 1.000 g of cellulose (oven-dried at 105 °C for 4 h and cooled in a non-hygroscopic desiccator) was treated with 5% NaOH (w/v) for 5 h (fiber to solution w/w ratio 1:30). The content was then cooled and neutralized with 10% H_2SO_4. The residual biomass was washed several times and treated for 5 h at room temperature with 2% H_2O_2 solution prepared in $NaHCO_3$−Na_2CO_3 buffer system of pH 9. The biomass was washed multiple times and dried at 105 °C until a constant weight was obtained. The weight difference was used to calculate cellulose content. Three independent measurements were made for each sample.

For the determination of lignin, 1.000 g of the extractive free paper sample was treated with 72% H_2SO_4 (sample to acid ratio 1:12.5 w/v) with careful shaking for 2 h. The top content was removed after several dilutions and washings. The residue was filtered and dried at 105 °C until a constant weight was obtained. The weight difference was used to calculate lignin content. Three independent measurements were made for each sample.

To determine the hemicellulose content, 1.000 g of the extractive free sample was boiled in 0.5 M NaOH for 4 h. The content was neutralized after several washings with distilled water and dried at 105 °C until a constant weight was obtained. The weight difference was used to calculate hemicellulose content. Three independent measurements were made for each sample.

To determine the ash content, 1.000 g of the moisture-free paper sample was burnt in an electric muffle furnace at 550 ± 10 °C. The weight difference was used to calculate ash content in percentage. Three independent measurements were made for each sample.

2.2.3. XRD, SEM, AFM, and FTIR Measurements. X-ray diffraction (XRD) data were collected in the 2θ range of 5−40° at a scan rate of 0.25°/min and a step size of 0.02° using a Rigaku Miniflex 600 X-ray diffractometer (operating at a 20 kV voltage and a 2 mA current). The X-ray source was the Cu Kα line (λ = 1.540 Å).

Scanning electron microscopy (SEM) images were collected using a field-emission electron probe microanalyzer (EPMA, JEOL JXA-8530F) with SDD X-ray energy-dispersive spectrometer (EDS). For each sample, four to six SEM images were collected at 100−5000× magnifications. Fiber width measurement was carried out using open-source software (ImageJ, NIH,

https://doi.org/10.1021/acsomega.2c04398
ACS Omega 2022, 7, 32717−32726

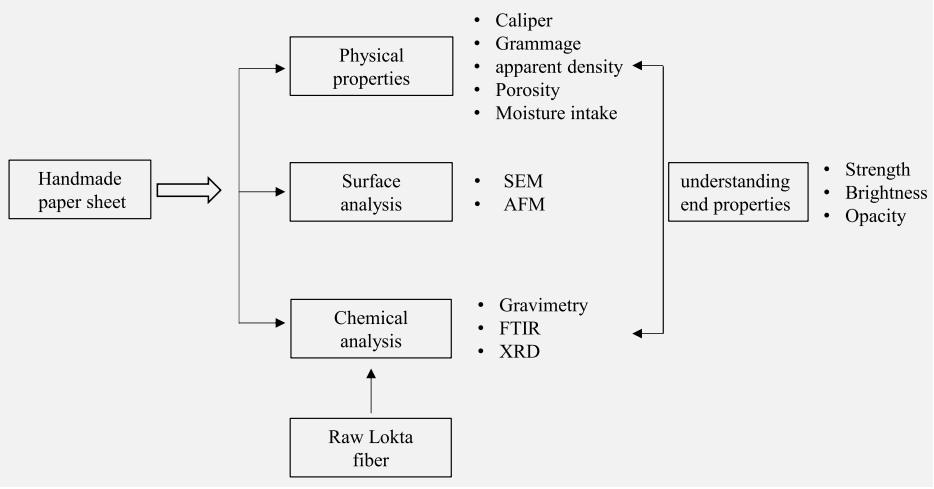

Figure 1. Schematic figure for the conceptual framework used in this work.

Table 1. Physical Properties of Paper Samples

paper	caliper (μm), n = 6	grammage (g/m^2), n = 6	apparent density (g/cm^3)	porosity (ε %)	moisture content (%), n = 3	Cobb 60 (g/m^2), n = 5
P1	207.2 ± 26.4	50.2 ± 2.4	0.25 ± 0.03	83.5 ± 2.3	4.3 ± 0.1	114.9 ± 14.0
P2	196.5 ± 11.1	74.7 ± 4.7	0.38 ± 0.03	74.4 ± 1.9	4.7 ± 0.3	154.2 ± 20.1
P3	462.5 ± 55.1	155.0 ± 11.7	0.34 ± 0.07	77.1 ± 4.5	5.3 ± 0.0	351.2 ± 14.0
P4	143.2 ± 2.8	47.7 ± 1.5	0.33 ± 0.01	77.6 ± 0.8	6.7 ± 0.8	96.4 ± 5.9
P5	158.0 ± 10.7	26.3 ± 1.9	0.17 ± 0.01	88.8 ± 1.1	5.8 ± 0.3	92.0 ± 9.1
P6	166.0 ± 13.2	54.6 ± 5.0	0.33 ± 0.02	77.7 ± 3.8	5.6 ± 1.2	128.5 ± 9.6
P7	274.8 ± 24.2	128.7 ± 5.3	0.47 ± 0.06	68.4 ± 3.2	6.±0.6	221.4 ± 10.4
P8	674.0 ± 110.7	128.9 ± 7.8	0.19 ± 0.05	86.9 ± 1.8	7.3 ± 0.4	411.4 ± 26.6
P9	91.8 ± 11.4	17.7 ± 2.4	0.20 ± 0.04	86.8 ± 2.8	5.9 ± 0.8	52.3 ± 4.6
P10	122.3 ± 8.3	28.7 ± 1.3	0.24 ± 0.01	84.2 ± 0.7	4.9 ± 0.5	63.1 ± 6.3

USA). Atomic force microscopy (AFM) was conducted using Agilent 5500.

The IR spectra were collected in the range of 4000−400 cm^{-1} in an attenuated total reflection (ATR) mode using a Fourier transform infrared spectrometer (FTIR) (ABB Bomen, MB100, Canada). The spectra were measured at the spectral resolution 4 cm^{-1}. To obtain a good signal-to-noise ratio, each reported spectrum is reported as an average of 16 optical scans. Prior to FTIR measurements, the paper samples were conditioned in standard atmosphere of 23 °C and 50% RH for 24 h and kept in a non-hygroscopic desiccator.

The basic idea or conceptual framework of this work is summarized in Figure 1.

3. RESULTS AND DISCUSSION

3.1. Basic Physical Properties. The basic physical parameters for all paper samples are provided in Table 1, and the individual data sets are provided in Tables S1−S3. The mean thickness values (caliper) for the paper samples ranged from ∼90 μm (P9) to 675 μm (P8). Similarly, grammage ranged from ∼20 g/m^2 (P9) to 150 (P3). A good positive correlation (r = 0.83) was observed between these two parameters. The wide variation in grammage indicates that these papers are intended for different purposes. Paper sheets having grammage at or below 50 are normally used for printing purpose, and the paper of higher grammage is used to design other value-added products such as photo albums and gift boxes.

We measured caliper with a digital micrometer having a resolution of 10 μm. For example, the caliper of sample P1 ranged from 180 to 254 μm (mean = 207.2 ± 26.4 μm). The large variation in caliper indicates that HP samples have non-uniform thickness. Handmade paper samples are generally fabricated following the chemical-mechanical method of fiber processing, which mostly results in long fiber (<1 mm). The long fibers have strong propensity to *floc* formation during the paper-making process, which results in thickness variation.[19,27]

We also calculated the apparent density (g/cm^3) of all the paper samples by taking the ratio of grammage (g/m^2) to thickness (μm). The apparent density ranged from ∼0.20 (P8 and P9) to 0.50 (P7) g/cm^3 (Table 1). Apparent density of paper also includes the volume occupied by air or open space in the paper. Therefore, apparent density is always lower than true density. The apparent density of machine-made and commercially available paper sheet has been reported to be higher (0.5−0.8 g/cm^3) than that of Lokta papers.[3,28] The low apparent density suggests that HPs are lightweight paper.

The apparent porosity of paper can be estimated from known density of paper network and cellulose.[29−32] In this work, apparent porosity was calculated using eq 1 (reprinted with permission from ref 29, copyright Elsevier 2012).

$$\varepsilon(\%) = \left[1 - \frac{\rho_{adp}}{\rho_{cf}}\right] \times 100 \quad (1)$$

where ρ_{adp} and ρ_{cf} are apparent density of the paper network and density of cellulose fiber, respectively. A cellulose fiber density of 1.49 g/cm^3 was used for the calculation.[33] Apparent porosity was found to be in the range of ∼69% (P7) to 89% (P5). A perfect negative correlation was observed between apparent density and

https://doi.org/10.1021/acsomega.2c04398
ACS Omega 2022, 7, 32717−32726

Table 2. Mechanical and Optical Properties of all the Paper Samples

	tensile strength, kN/m		tensile index, Nm/g				
samples	LD	CD	LD	CD	brightness	opacity	RBA
P1	0.6 ± 0.1	0.4 ± 0.1	12.7 ± 1.6	8.4 ± 1.3	66.8 ± 0.4	92.9 ± 0.5	0.028
P2	2.05 ± 0.1	1.9 ± 0.0	27.4 ± 1.1	25.4 ± 0.5	61.9 ± 0.7	97.1 ± 0.4	0.069
P3	2.02 ± 0.4	1.7 ± 0.1	13.0 ± 2.8	10.8 ± 0.8	65.1 ± 0.3	97.7 ± 0.2	0.052
P4	0.7 ± 0.0	0.6 ± 0.1	15.9 ± 0.5	12.1 ± 1.6	62.7 ± 0.5	95.3 ± 0.4	0.054
P5	0.03 ± 0.0	0.02 ± 0	1.2 ± 0.4	0.7 ± 0.1	61.8 ± 0.1	86.4 ± 2.2	0.013
P6	1.2 ± 0.1	1.08 ± 0.1	18.3 ± 1.2	16.9 ± 0.9	63.8 ± 0.7	95.4 ± 0.4	0.052
P7	2.9 ± 0.0	2.69 ± 0.1	22.4 ± 0.3	21.1 ± 1.0	61.4 ± 0.7	97.5 ± 0.3	0.103
P8	1.5 ± 0.0	1.25 ± 0.1	11.7 ± 0.4	9.7 ± 0.9	55.6 ± 0.3	97.8 ± 0.4	0.017
P9	0.3 ± 0.0	0.22 ± 0.0	14.3 ± 1.2	12.2 ± 0.9	59.6 ± 0.5	79.5 ± 3.4	0.019
P10	0.4 ± 0.0	0.34 ± 0.0	15.2 ± 1.1	11.4 ± 0.8	66.9 ± 0.4	87.4 ± 1.7	0.027

porosity ($r = -1$). In paper making, low apparent density (high porosity) arises due to the long and stiff fibers, insufficient refining, absence of fillers and fines, insufficient or no calendaring, and their combinations,[28] which could explain the low apparent density of handmade papers. Low apparent density in the range of 0.2−0.5 g/cm^3 was also reported in laboratory-made handmade paper samples.[6,10,11]

Equilibrium moisture content (EMC) of the paper samples ranged from ∼4.3% (P1) to 7.3% (P8). Similar values of moisture content were reported for cellulose-based paper sheet.[28] The Cobb 60 value is the most used parameter to measure the water absorption tendency of a paper sheet. Cobb 60 is the measurement of amount/weight of water absorbed in 60 s by 1 square meter of paper under 1 cm of water. The Cobb value depends on fiber chemical composition, fiber morphology and organization, and caliper. The Cobb sizing ranged from ∼50 (P9) to 410 g/m^2 in the samples we tested. The wide variation in Cobb 60 could be linked to the difference in chemical composition of the paper samples (reported in Table 3) and a small difference in fiber morphology and organization (SEM images in Figure 4). A Cobb 60 value of handmade paper shows strong positive correlation with the caliper ($r = +0.97$) and grammage ($r = +0.92$). It is possible that in thick and porous paper, the retained water could be difficult to remove with mechanical pressing, with a 10 kg roller in the experiment, leading to a high Cobb 60 value.

Table 3. Chemical Composition Data for the Paper Samples and Raw Lokta Fiber

samples	cellulose (%)	hemicellulose (%)	lignin (%)	ash (%)
P1	66.0 ± 1.7	23.5 ± 4.0	3.9 ± 0.5	7.8 ± 0.0
P2	67.4 ± 7.2	25.9 ± 0.4	5.7 ± 0.2	4.5 ± 0.7
P3	83.6 ± 6.5	11.4 ± 3	2.0 ± 0.5	3.5 ± 0.6
P4	81.7 ± 4.4	11.3 ± 4.0	2 ± 0.7	3.6 ± 0.5
P5	73.1 ± 2.8	19.5 ± 1.4	9.8 ± 0.3	7.7 ± 0.1
P6	80.4 ± 3.9	12.1 ± 2.2	5.4 ± 0.5	6.6 ± 0.4
P7	75.7 ± 3.8	14.1 ± 1.7	7.5 ± 0.7	3.5 ± 0.4
P8	71.4 ± 1.1	20.8 ± 0.3	9.3 ± 1.5	3.6 ± 0.1
P9	76.2 ± 1.8	18.2 ± 1.0	7.4 ± 0.5	7.1 ± 0.5
P10	75.7 ± 1.1	13.7 ± 2.1	7.9 ± 1.3	3.5 ± 0.6
raw fiber	36.8 ± 1.0	44.0 ± 1.0	19.2 ± 1.0	2.6 ± 0.2

3.2. Optical Properties. Brightness and opacity are the important optical parameters of paper. With blue light illumination, a yellowish paper reflects less light or absorbs more light. Therefore, higher brightness is the indicator of lower yellowness of paper. Brightness of the paper sample is determined by the degree of bleaching and surface smoothness. For bleached and gazed commercial printing paper, ISO brightness as high as 100% is reported.[28] The brightness of the paper samples ranged from 56% (P8) to 67% (P1 and P10) (Table 2 and Figure S1).

Brightness of paper and pulp samples depends on several parameters such as lignin and coloring impurity content and microscopic surface structures.[28] Relatively lower brightness values for the handmade paper samples could be due to unbleached pulp used in paper making and/or lower quality water and reagents used in the pulping process. The brightness and lignin content data for the paper samples (Tables 2 and 3) showed a fairly good negative correlation ($r = -0.51$).

Opacity measures the ability of paper to mask an object located on the back of the sheet. For double-sided printing, a high opacity paper is required to read the front page without being distracted by the characters or images on the back side and to avoid the strike through. In bulky paper sheet, microscopic air spaces or pores reflect more blue light, leading to high opacity.[28] In our study, opacity of the paper samples ranged from ∼83% (P9) to 98% (P2, P7, and P8) (Table 2). Higher opacity could be due to low apparent density or high porosity of the papers. We found a moderate positive correlation ($r = +0.68$) between opacity and apparent density.

3.3. Mechanical Properties. We measured tensile strength and tensile index of all the paper samples in two directions: along and across the length of the wooden frame or paper molds. For easy comparison hereunder, we label these directions LD and CD. In machine-made paper, there directions are commonly labeled as machine direction (MD) and cross direction (CD). The tensile strength along the LD ranged from 0.03 (P5) to 2.9 (P7) kN/m with the corresponding CD values ranged from 0.02 to 2.7 kN/m (Table 2 and Figure S1). In handmade paper making, pulp is added to a rectangular wooden mesh/frame (paper molds, size 40 cm × 60 cm) over the pool of water, and the slurry is gently dispersed by shaking the wooden frame along the length. This could result in partial alignment of fibers along the frame length and explain the observed difference in strength in two directions.

Tensile strength is the maximum stress applied per unit width (N/m or kN/m) of paper to break the paper strip. During printing and other applications such as preparation of gummed paper tape, a paper sheet can be subjected to different levels of stress. A paper having low tensile strength can lead to web breaking in these activities.[28] Moderately high values of tensile strength values indicate that web breaking during printing is less likely in the handmade paper samples reported here.

https://doi.org/10.1021/acsomega.2c04398
ACS Omega 2022, 7, 32717−32726

We also measured the tensile strength index, which is the grammage normalized tensile strength, values along LD and CD directions. Tensile index of the paper samples along the LD and CD ranged from 1.2 (P5) to 27.5 (P2) Nm/g and 0.7 (P5) to 25.4 (P2) Nm/g, respectively (Table 2). For all samples, the LD values are significantly higher than CD ($p < 0.05$) with an average LD: CD ratio of ~1.1 (P7) to 2 (P7). This indicates that the fiber orientation along two directions is different. An MD/CD ratio of ~1.5−5 is reported in machine-made paper.[28] This observation suggested that fiber orientation in handmade paper is lower than in machine-made paper.

Tensile strength of paper-based materials depends on several factors including strength of individual fiber, fiber length, and fiber-to-fiber contact and bonding. Considering a paper sheet as a multi-layered composite structure of two-dimensional fibrous networks not interwinded between layers, the amount of contact between two layers defined in terms of relative bonding area (RBA) can be calculated.[32,34] From the information on fractional porosity (ε) and number of fiber layers (n), which is defined as the ratio of caliper to fiber diameter, a rough estimate of RBA can be made.[32] The RBA values for all the paper samples are provided in Table 2. A fiber diameter of 10 μm was used in the estimation of RBA.

For fibers of the same length, coarseness, cross section perimeter, and bonding strength, the tensile strength of a fiber sheet is directly proportional to relative bonding area.[35,36] Microscopy images shown in the later section support the fact that the fiber morphology (length, width, and coarseness) is similar in the paper samples studied here. Interestingly, RBA values and measured tensile strength (Table 2) showed a fairly good positive correlation (r = +0.83) (Figure 2). Considering

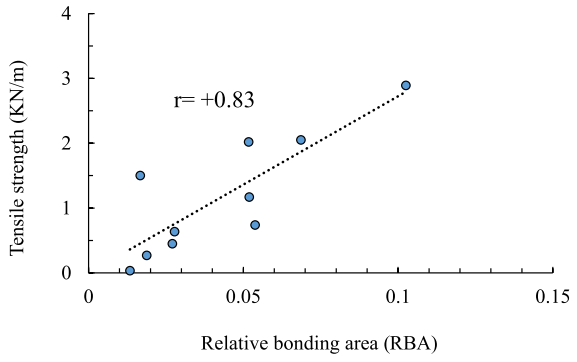

Figure 2. Plot of tensile strength versus relative bonding area. The dotted line is the liner fit to the measured data.

the abovementioned discussion, the lowest and highest tensile strength values for P5 and P7 could be due to the lowest and highest RBA values, respectively. Variation in tensile strength could be partly linked to variation in fiber-to-fiber bonding strength resulted from the difference in chemical composition (Table 3) in the paper sheets.

3.4. Chemical Analysis. We also measured cellulose, hemicellulose, lignin, and ash content in all the samples and in raw Lokta fiber (Table 3). The mean values (n = 3) for cellulose, hemicellulose, lignin, and ash content ranged from ~66 to 84, 11 to 26, 2 to 10, and 3 to 8%, respectively. As compared to paper samples, raw Lokta fiber showed a significantly high amount of lignin (~19%) and hemicellulose (~44%) and low amount of cellulose (~37%). In fiber processing, lignin and hemicellulose are partially removed, thereby resulting in a net increase in cellulose content.[26,37] This explains the higher amount of cellulose or lower lignin and hemicellulose observed in the paper samples. The difference in chemical composition in the paper samples could be due to variability in fiber processing and or different types of fibers used in making the paper samples.

3.5. FTIR and XRD Study. The FTIR data of all the paper samples and Lokta fiber are provided in Figure 3A. The spectra look similar in shape with a small difference in the relative peak intensities. We made the spectral assignments on the basis of literature-provided information.[30,38−41] The broad peak in the range of 3000−3600 cm^{-1} (with three weak peaks/shoulders) is attributed to the O−H stretching of cellulose. The weak peak ~2900 cm^{-1} is due to the aliphatic C−H stretching vibration in hemicellulose and cellulose.[38] Peak ~1735 cm^{-1} arises due to acetyl or ester C═O groups of hemicellulose or lignin,[30] and the peak ~1630 cm^{-1} originates from C═O stretching of conjugated lignin.[30,42] These peaks are relatively stronger in raw Lokta fiber. This observation suggested that hemicellulose and lignin are partially removed in pulping. A weak peak at 1250 cm^{-1} corresponds to C−O stretching of acetyl groups of hemicellulose and cellulose.[43] The peak is weaker in paper samples, suggesting that fiber processing during paper making resulted in removal of hemicellulose. These observations are consistent with the chemical analysis data reported in Table 3. A summary of the observed IR peaks and their interpretation is provided in Table 4.

Crystalline natural cellulose exists in two allomorphs I_α and I_β. I_β allomorph is reported to be thermodynamically more stable. Interestingly, characteristic peaks of crystalline cellulose I_β (weak peaks at ~710 and 3270 cm^{-1})[41,44,45] and amorphous cellulose (weak peak ~660 cm^{-1} and a weak broad shoulder ~3420 cm^{-1})[40] are also observed in all paper samples and raw fiber. We did not see the characteristic features for I_α in all the samples, which are reported to be ~3240 and 750 cm^{-1}.[44] The composition of I_α and I_β is reported to be species-dependent. Also, due to meta-stability of I_α, it could change to the I_β form during pulping.[41] Since I_α peaks are also absent in raw fiber, the later possibility could be ruled out.

The absorption intensity ratio of different IR bands is used to obtain information on hydrogen bond intensity (HBI) in cellulose-based samples.[46−49] Hydrogen bond intensity is related to the amount of bound water and structural flexibility. Generally, crystallinity decreases as HBI increases.[47] We used the absorption ratio of bands at ~3336 and 1320 cm^{-1} (A_{3336}/A_{1320}) to calculate HBI.[48,49] The HBI ranged from ~1.2 to 1.5 (Table 5). HBI depends on the type of fiber and fiber-processing parameters. Therefore, it is not surprising to see the observed differences in HBI in the samples. For reference, HBI in the range of 1.4−1.8 is reported for different cellulose samples.[47−49]

We also measured the XRD data of all the paper samples and raw fiber (Figure 3B). The peak at 2θ values of ~21.5 and ~15.5° originates from (200) and (1−10/110) planes of crystalline phase cellulose I, respectively.[50,51] A broad background underlying the peaks is attributed to the amorphous phase.[50,52] We also calculated the XRD crystallinity index (CI) following eq 2 (reprinted with permission from ref 26, copyright Springer Nature 2022).

$$\mathrm{CI} = \left(\frac{A_t - A_{am}}{A_t}\right) \times 100 \tag{2}$$

where A_t is the integrated intensity of both crystalline and amorphous phases and A_{am} is the intensity of amorphous phase

https://doi.org/10.1021/acsomega.2c04398
ACS Omega 2022, 7, 32717−32726

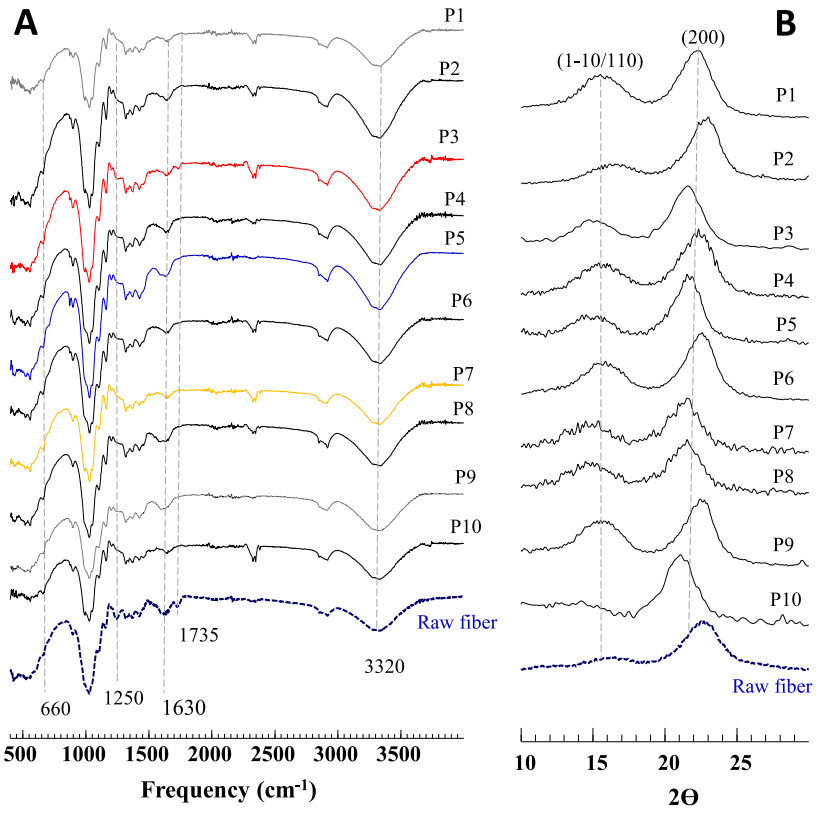

Figure 3. FTIR and XRD data. (A) FTIR data of paper samples P1−P10 and raw fiber. Spectra are overlaid vertically for easy compassion. Important peaks are indicated by dotted vertical lines. (B) XRD data of the paper samples. Reflection planes at 2θ values of ∼15.5 and 21.5° are indicated in parenthesis. For easy comparison, spectra are overlaid in the vertical direction.

Table 4. IR Peaks and Their Spectral Assignment[a]

peak position (cm^{-1})	relative intensity	assignment
3000−3600	S	O−H (symmetric) stretching of cellulose
2900	M	aliphatic C−H (asymmetric) stretching of cellulose and hemicellulose
2850	M	aliphatic C−H (symmetric) stretching of lignin and cellulose
2330, 2350	M	carbonate impurities
1735	W	C═O stretch (non-conjugated) hemicellulose and lignin
1630	M	C═O stretch (conjugated) lignin
1590	M	aromatic ring vibration and C═O stretch lignin
1510	W	aromatic ring vibration lignin
1465	W	C−H deformation lignin
1450	W	O−H in-plane bending cellulose and hemicellulose
1430	W	C−H in-plane deformation lignin
1370	M	C−H bending cellulose, hemicellulose, and lignin
1200	M	O−H bending of cellulose and hemicellulose
1250	W	C−O stretching of acetyl groups of hemicellulose and cellulose
1160	S	C−O−C asymmetrical stretching cellulose and hemicellulose
1030, 1000	S	C−O, C═C, and C−C−O stretching of lignin, cellulose, and hemicellulose
900, 875	M	glycosidic linkage hemicellulose and cellulose
710	W	O−H out of plane bending of crystalline cellulose I_β
660	W	O−H out of plane bending of amorphous cellulose

[a]S = strong, M = medium, and W = weak.

only. We carried out Gaussian fitting in the 2θ range of 10−30° to calculate A_t, A_{am}, and CI. The CI in the paper samples ranged from ∼62 to 85% (Table 4). In the raw fiber, CI was found to be 58.5%. The CI depends on the source of cellulose biomass and processing parameters, which explains the observed differences in the samples P1−P10. If a fiber is treated with alkali in the paper-making process, lignin is removed from the interfibrillar region, resulting in reorganization of the cellulose chain and an increase in the crystallinity index.[50,51] This explains the higher crystallinity index observed in all paper samples than in raw fiber. For reference, CI in the range 20−97% is reported for different cellulose samples.[47−49] We also found a good negative correlation between HBI and CI (r = −0.83). This observation is consistent with literature study.[47]

3.6. SEM Imaging of the Paper Samples. The representative SEM images of the paper samples are provided in Figure 4A−J. In the images, individual fibers are randomly arranged to form interwoven networks. The presence of long (>1 mm) and interconnected fibers provides strength to the paper sheet. It is interesting to find a few fibrillated, damaged, and curled fibers in images of paper samples P1, P2, and P10 (Figure 4A,B,J). Such fibers can be formed due to mechanical and chemical forces during fiber processing and paper making.

Fiber width is an important parameter to measure fiber intactness and strength of a paper sheet. A paper sheet having a large fraction of collapsed fiber can have lower strength.[12,28] We measured the fiber width in all the samples. The mean, minimum, and maximum fiber width values obtained from 100 measurements in each sample were found in the range of 9−11, 4−6, and 18−26 μm, respectively. The mean fiber width distribution was insignificant in all the samples ($p < 0.05$). As an

https://doi.org/10.1021/acsomega.2c04398
ACS Omega 2022, 7, 32717−32726

Table 5. Hydrogen Bonding Intensity (HBI) and CI of the Paper Samples

parameters	P1	P2	P3	P4	P5	P6	P7	P8	P9	P10
HBI	1.48	1.52	1.33	1.38	1.21	1.50	1.52	1.34	1.22	1.19
CI	70.7	65.4	72.9	62.4	83.8	72.6	62.2	70.2	83.6	84.5

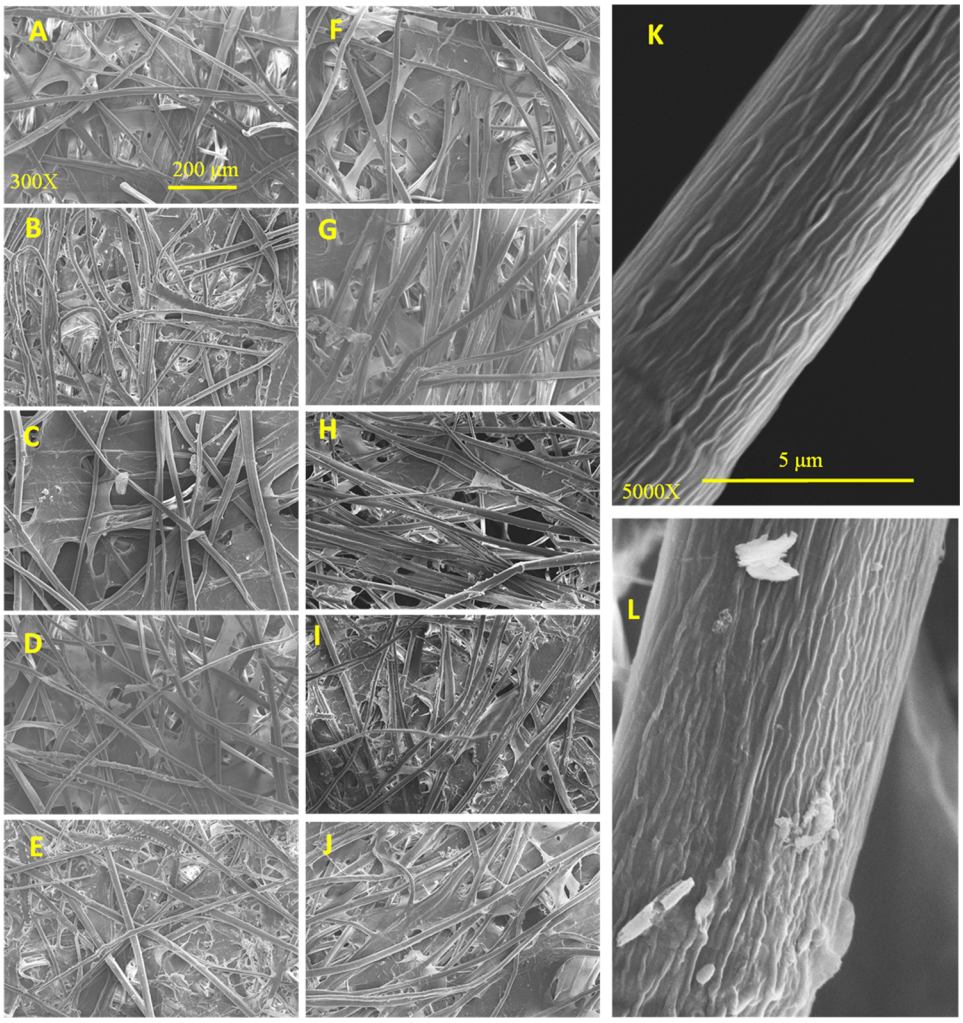

Figure 4. (A) SEM micrograph of the paper samples. (A–J) Images of paper samples P1–P10 taken at 300×, respectively. The scale bar of 200 μm shown in (A) also applies for (B–J). Images of individual fiber taken at 5000× for samples P3 (K) and P8 (L). The scale bar of 5 μm shown in (K) applies for (L).

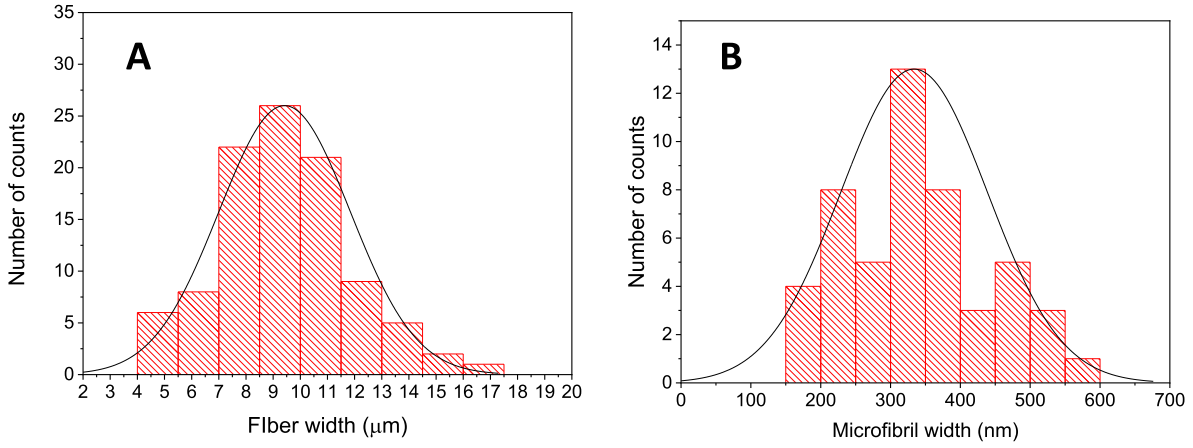

Figure 5. Fiber and microfibril width distribution. (A) Fiber width (n = 100) and (B) microfibril width distribution in P3 (n = 50). In both figures, the solid curve shows normal distribution.

https://doi.org/10.1021/acsomega.2c04398
ACS Omega 2022, 7, 32717−32726

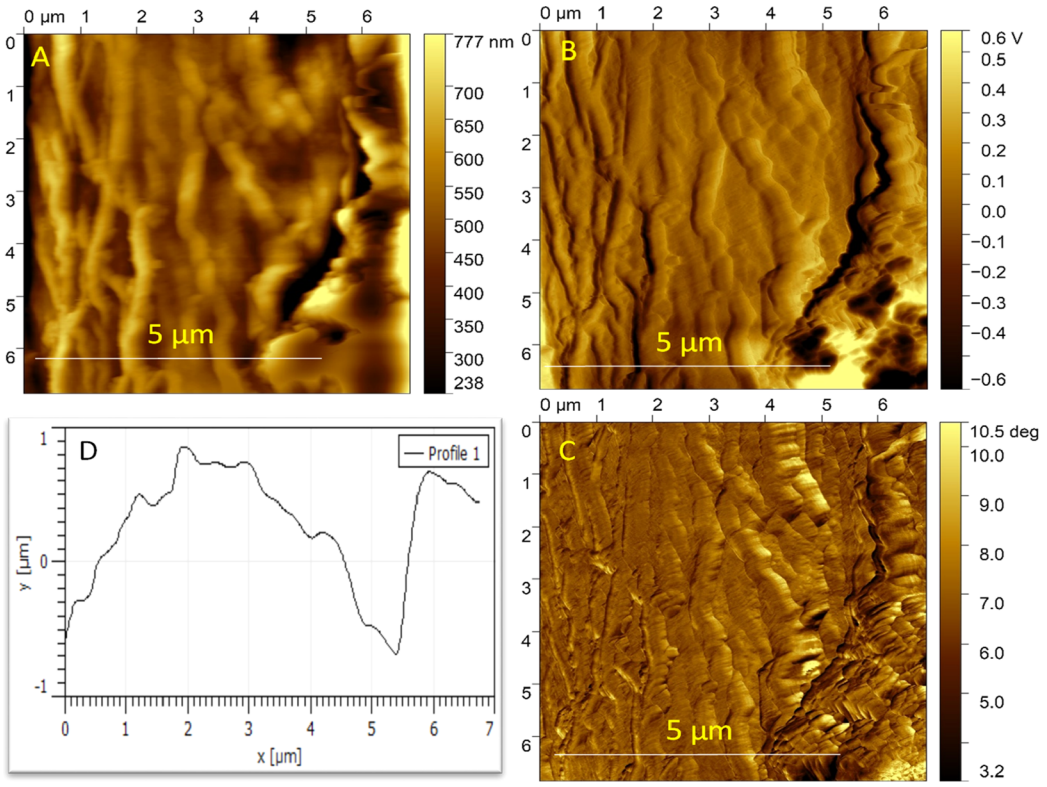

Figure 6. AFM topography (A), amplitude (B), and phase (C) images of small regions with a cellulose fiber and profile (D) along the line labeled in (A).

example, the fiber width distribution of sample P3 is provided in Figure 5A. During fiber processing, lumen or cell wall in some of the fibers can collapse to from ribbon-like flexible fibers. The collapsed fiber can have high apparent width.[14,53] Also, some of the fibers may not be separated or remain attached to form a bundle which can result in high apparent width. These reasonings explain observation of high apparent width (≥20 μm) in some of the fibers. This fraction was found to be ≤5% in all the samples.

A zoomed-in image of individual fiber is provided in Figure 4K,L. It is interesting to see individual microfibrils that run almost straight along the lengths of fiber. We found mean microfibril width in the samples in the range of 250−450 nm (n = 50). As an example, the width distribution profile of sample P3 is provided in Figure 5B. The microfibrils are visible due to removal of gummy materials such as lignin and hemicellulose from the fiber surface during fiber processing. Almost parallel arrangement of the microfibrils (Figure 4K,L) can provide excellent strength to individual fiber and to the fiber web.

Tensile strength of a paper sheet depends partly on fiber surface roughness. Microscopic or sub-microscopic structures/roughness at the individual fiber level can lead to increased fiber−fiber bonding and increased strength.[12] To explore this, we carried out AFM imaging in a selected sample, the thinnest sample P9 (Figure 6A−D). The surface roughness and microfibrils are clearly visible in the images. A line profile on the topographic image shows a roughness of ∼±700 nm (Figure 6D). These surface structures could be partly responsible for the paper strength.

3.7. Further Implications of the Research. Present study was intended to investigate material properties of HPs down to the sub-microscopic level and explains the observed difference in mechanical and optical properties. The paper samples had low apparent density (i.e., high porosity), thickness variation, and low brightness. Eco-friendly and low-cost strategies to improve these properties would be useful for handmade paper industries. Enzymatic bleaching of the pulp using locally isolated microbial cultures could be explored to increase the brightness. Calendaring of paper sheet by a locally designed handmade machine would be useful to improve high porosity and thickness variation issues.

In the future, handmade paper or raw Lokta fiber could be used as a starting material for the synthesis/fabrication of useful nanomaterials such as nanocellulose,[54−56] antimicrobial cellulose film,[57] and micro- and nanocomposite materials for chemical sensing and filtering applications.[58−60]

4. CONCLUSIONS

To summarize, we measured several physical and chemical parameters of 10 different Nepali handmade paper samples. The mean caliper, grammage, and apparent density values in the paper samples ranged from ∼90 to 700 μm, 50 to 150 g/m^2, and 0.2 to 0.4 g/cm^3, respectively. The optical brightness, tensile strength, and tensile index values ranged from 56 to 67%, 30 to 2900 N/m, and 1 to 27 Nm/g, respectively. The tensile strength along the length direction (LD) was found to be significantly higher than in cross direction (CD) ($p < 0.05$). These properties suggested that HP is lightweight paper, having intermediate yellowness but medium to high tensile strength. In all the samples, characteristic features of crystalline and amorphous cellulose phases were observed both in FTIR and XRD data. SEM micrographs of the paper sheet revealed interconnecting networks of long cellulose fibers. Imaging of the individual fiber surface revealed almost parallel arrangement of microfibrils.

https://doi.org/10.1021/acsomega.2c04398
ACS Omega 2022, 7, 32717−32726

These properties explain the observed mechanical properties of the paper samples.

■ ASSOCIATED CONTENT

Supporting Information

The Supporting Information is available free of charge at https://pubs.acs.org/doi/10.1021/acsomega.2c04398.

Individual data sets (as measured) for caliper, grammage, tensile strength, tensile index, brightness, opacity, and chemical composition (PDF)

■ AUTHOR INFORMATION

Corresponding Authors

Bhoj Raj Gautam − *Department of Chemistry, Physics and Materials Science, Fayetteville State University, Fayetteville, North Carolina 28301, United States*; Email: bgautam@uncfsu.edu

Bhanu Bhakta Neupane − *Central Department of Chemistry, Tribhuvan University, Kathmandu 44613, Nepal*; orcid.org/0000-0003-0731-2552; Email: bbneupane@cdctu.edu.np

Authors

Girja Mani Aryal − *Central Department of Chemistry, Tribhuvan University, Kathmandu 44613, Nepal; Research Centre for Applied Science and Technology, Tribhuvan University, Kathmandu 44613, Nepal*

Krishna Prasad Kandel − *Central Department of Chemistry, Tribhuvan University, Kathmandu 44613, Nepal*

Ram Kumar Bhattarai − *Center for Analytical Sciences, Kathmandu Institute of Applied Sciences, Kathmandu 44600, Nepal*

Basant Giri − *Center for Analytical Sciences, Kathmandu Institute of Applied Sciences, Kathmandu 44600, Nepal*

Menuka Adhikari − *Department of Chemistry, Physics and Materials Science, Fayetteville State University, Fayetteville, North Carolina 28301, United States*

Alisha Ware − *Department of Chemistry, Physics and Materials Science, Fayetteville State University, Fayetteville, North Carolina 28301, United States*

Shubo Han − *Department of Chemistry, Physics and Materials Science, Fayetteville State University, Fayetteville, North Carolina 28301, United States*

Gibin George − *Department of Chemistry, Physics and Materials Science, Fayetteville State University, Fayetteville, North Carolina 28301, United States*

Zhiping Luo − *Department of Chemistry, Physics and Materials Science, Fayetteville State University, Fayetteville, North Carolina 28301, United States*; orcid.org/0000-0002-8264-6424

Complete contact information is available at: https://pubs.acs.org/10.1021/acsomega.2c04398

Notes

The authors declare no competing financial interest.

■ ACKNOWLEDGMENTS

This work was supported by the University Grants Commission, Nepal (to B.B.N. and K.P.K., grants # FRG-6/77-S&T-3 and PhD-76/77-S&T-10) and by NSF DMR 1827731 and EIR ECCS 1900837 (B.R.G., S.H. and Z.L.).

■ REFERENCES

(1) Hubbe, M. A.; Bowden, C. Handmade Paper: A Review of Its History, Craft, and Science. *BioResources* **2009**, *4*, 1736−1792.

(2) Biggs, S.; Messerschmidt, D. Social Responsibility in the Growing Handmade Paper Industry of Nepal. *World Dev.* **2005**, *33*, 1821−1843.

(3) ITC. *Nepal National Center Export Strategy: Handmade Paper and Paper Products 2017−2021*; International Trade Center, Government of Nepal, 2017; pp 1−124.

(4) Banjara, G. *Handmade Paper in Nepal: Upgrading with Value Chain Approach*; GTZ/PSP-RUFIN, 2007.

(5) Poudyal, A. Sustainability of Local Hand-Made Paper (Nepali Kagat) Enterprises: A Case Study of Dolakha District. *J. For. Livelihood* **2004**, *4*, 64−69.

(6) Mejouyo, P. W. H.; Nkemaja, E. D.; Beching, O. R.; Tagne, N. R.; Kana'a, T.; Njeugna, E. Physical and Tensile Properties of Handmade Sida Rhombifolia Paper. *Int. J. Biomater.* **2020**, *2020*, 1.

(7) Kumar, A.; Singh, B. P.; Jain, R. K.; Sharma, A. K. Banana Fibre (Musa Sapientum): A Suitable Raw Material for Handmade Paper Industry via Enzymatic Refining. *Int. J. Eng. Res.* **2013**, *2*, 1338−1350.

(8) Sottile, F.; Modica, A.; Rosselli, S.; Catania, C. A.; Cavallaro, G.; Lazzara, G.; Bruno, M. Hand-Made Paper Obtained by Green Procedure of Cladode Waste of Opuntia Ficus Indica (L.) Mill. from Sicily. *Nat. Prod. Res.* **2021**, *35*, 359−368.

(9) Arafat, Km.; Nayeem, J.; Quadery, A. H.; Quaiyyum, M. A.; Jahan, M. S. Handmade Paper from Waste Banana Fibre. *Bangladesh J. Sci. Ind. Res.* **2018**, *53*, 83−88.

(10) Reddy, K. O.; Uma Maheswari, C.; Shukla, M.; Muzenda, E. Preparation, Chemical Composition, Characterization, and Properties of Napier Grass Paper Sheets. *Sep. Sci. Technol.* **2014**, *49*, 1527−1534.

(11) Marrakchi, Z.; Khiari, R.; Oueslati, H.; Mauret, E.; Mhenni, F. Pulping and Papermaking Properties of Tunisian Alfa Stems (Stipa Tenacissima)—Effects of Refining Process. *Ind. Crops Prod.* **2011**, *34*, 1572−1582.

(12) Johansson, A. Correlations between Fibre Properties and Paper Properties. M.S. Thesis, 2011.

(13) Lundberg, M.; Norgren, M.; Edlund, H. Validation of Crill Measurements in a High-Yield Pulp Refining Process for Improved Fines Material Control. *Nord. Pulp Pap. Res. J.* **2018**, *33*, 200−209.

(14) Hubbe, M. A. Difficult Furnishes. *Proc. TAPPI* **1999**, *99*, 1353−1367.

(15) Larsson, P. T.; Lindström, T.; Carlsson, L. A.; Fellers, C. Fiber Length and Bonding Effects on Tensile Strength and Toughness of Kraft Paper. *J. Mater. Sci.* **2018**, *53*, 3006−3015.

(16) Fischer, W.; Mayr, M.; Spirk, S.; Reishofer, D.; Jagiello, L. A.; Schmiedt, R.; Colson, J.; Zankel, A.; Bauer, W. Pulp Fines—Characterization, Sheet Formation, and Comparison to Microfibrillated Cellulose. *Polymers* **2017**, *9*, 366.

(17) Boufi, S.; González, I.; Delgado-Aguilar, M.; Tarrès, Q.; Pèlach, M. A.; Mutjé, P. Nanofibrillated Cellulose as an Additive in Papermaking Process: A Review. *Carbohydr. Polym.* **2016**, *154*, 151−166.

(18) Motamedian, H. R.; Halilovic, A. E.; Kulachenko, A. Mechanisms of Strength and Stiffness Improvement of Paper after PFI Refining with a Focus on the Effect of Fines. *Cellulose* **2019**, *26*, 4099−4124.

(19) Beghello, L. Some Factors That Influence Fiber Flocculation. *Nord. Pulp Pap. Res. J.* **1998**, *13*, 274−279.

(20) TAPPI. *Thickness (Caliper) of Paper, Paperboard, and Combined Board*, 1997. T411 om-97.

(21) TAPPI. *Grammage of Paper and Paperboard (Weight per Unit Area)*, 2012. T410 om-08.

(22) TAPPI. *Water Absorptiveness of Sized (Non-Bibulous) Paper, Paperboard, and Corrugated Fiberboard (Cobb Test)*; TAPPI, 2012. T441 om-09.

(23) Das, A. M.; Ali, A. A.; Hazarika, M. P. Synthesis and Characterization of Cellulose Acetate from Rice Husk: Eco-Friendly Condition. *Carbohydr. Polym.* **2014**, *112*, 342−349.

(24) Ayeni, A. O.; Oresegun, O. M.; Oladimeji, T. E. Compositional Analysis of Lignocellulosic Materials: Evaluation of an Economically

Viable Method Suitable for Woody and Non-Woody Biomass. *Am. J. Eng. Res.* **2015**, *4*, 14−19.
(25) Boopathi, L.; Sampath, P. S.; Mylsamy, K. Investigation of Physical, Chemical and Mechanical Properties of Raw and Alkali Treated Borassus Fruit Fiber. *Composites, Part B* **2012**, *43*, 3044−3052.
(26) Kandel, K. P.; Adhikari, M.; Kharel, M.; Aryal, G. M.; Pandeya, S.; Joshi, M. K.; Dahal, B.; Gautam, B.; Neupane, B. B. Comparative Study on Material Properties of Wood-Ash Alkali and Commercial Alkali Treated Sterculia Fiber. *Cellulose* **2022**, *29*, 5913.
(27) Lundell, F.; Söderberg, L. D.; Alfredsson, P. H. Fluid Mechanics of Papermaking. *Annu. Rev. Fluid. Mech.* **2011**, *43*, 195−217.
(28) Bajpai, P. Paper and Its Properties. *Biermann's Handbook of Pulp and Paper: Paper and Board Making*; Elsevier, 2018; Vol. *2*, pp 35−63.
(29) Tanpichai, S.; Sampson, W. W.; Eichhorn, S. J. Stress-Transfer in Microfibrillated Cellulose Reinforced Poly (Lactic Acid) Composites Using Raman Spectroscopy. *Composites, Part A* **2012**, *43*, 1145−1152.
(30) Tanpichai, S.; Witayakran, S.; Srimarut, Y.; Woraprayote, W.; Malila, Y. Porosity, Density and Mechanical Properties of the Paper of Steam Exploded Bamboo Microfibers Controlled by Nanofibrillated Cellulose. *J. Mater. Res. Technol.* **2019**, *8*, 3612−3622.
(31) Henriksson, M.; Berglund, L. A.; Isaksson, P.; Lindström, T.; Nishino, T. Cellulose Nanopaper Structures of High Toughness. *Biomacromolecules* **2008**, *9*, 1579−1585.
(32) Sampson, W. W. A Model for Fibre Contact in Planar Random Fibre Networks. *J. Mater. Sci.* **2004**, *39*, 2775−2781.
(33) Ehrnrooth, E. M. Change in Pulp Fibre Density with Acid-Chlorite Delignification. *J. Wood Chem. Technol.* **1984**, *4*, 91−109.
(34) Soszyński, R. M. Relative Bonded Area-A Different Approach. *Nord. Pulp Pap. Res. J.* **1995**, *10*, 150−151.
(35) Page, D. H. A. Theory for the Tensile Strength of Paper. *Tappi J.* **1969**, *52*, 674−681.
(36) Tao, J.; Liu, H. A Method to Determine Sheet Relative Bonded Area Using the Fiber Flexiblity Index. *Instrum. Sci. Technol.* **2011**, *39*, 161−172.
(37) Hashim, M. Y.; Amin, A. M.; Marwah, O. M. F.; Othman, M. H.; Yunus, M. R. M.; Chuan Huat, N. C. The Effect of Alkali Treatment under Various Conditions on Physical Properties of Kenaf Fiber. *J. Phys. Conf.*; IOP Publishing, 2017; Vol. *914*, p 012030. DOI: 10.1088/1742-6596/914/1/012030
(38) Poletto, M.; Ornaghi, H. L.; Zattera, A. J. Native Cellulose: Structure, Characterization and Thermal Properties. *Materials* **2014**, *7*, 6105−6119.
(39) Xu, F.; Yu, J.; Tesso, T.; Dowell, F.; Wang, D. Qualitative and Quantitative Analysis of Lignocellulosic Biomass Using Infrared Techniques: A Mini-Review. *Appl. Energy* **2013**, *104*, 801−809.
(40) Kondo, T.; Sawatari, C. A Fourier transform infra-red spectroscopic analysis of the character of hydrogen bonds in amorphous cellulose. *Polymer* **1996**, *37*, 393−399.
(41) Åkerholm, M.; Hinterstoisser, B.; Salmén, L. Characterization of the Crystalline Structure of Cellulose Using Static and Dynamic FT-IR Spectroscopy. *Carbohydr. Res.* **2004**, *339*, 569−578.
(42) Haque, M. M.; Hasan, M.; Islam, M. S.; Ali, M. E. Physico-Mechanical Properties of Chemically Treated Palm and Coir Fiber Reinforced Polypropylene Composites. *Bioresour. Technol.* **2009**, *100*, 4903−4906.
(43) Sinha, E.; Rout, S. K. Influence of Fibre-Surface Treatment on Structural, Thermal and Mechanical Properties of Jute. *J. Mater. Sci.* **2008**, *43*, 2590−2601.
(44) Sassi, J.-F.; Tekely, P.; Chanzy, H. Relative Susceptibility of the Iα and Iβ Phases of Cellulose towards Acetylation. *Cellulose* **2000**, *7*, 119−132.
(45) Sugiyama, J.; Persson, J.; Chanzy, H. Combined Infrared and Electron Diffraction Study of the Polymorphism of Native Celluloses. *Macromolecules* **1991**, *24*, 2461−2466.
(46) Xiao, L.-P.; Lin, Z.; Peng, W.-X.; Yuan, T.-Q.; Xu, F.; Li, N.-C.; Tao, Q.-S.; Xiang, H.; Sun, R.-C. Unraveling the Structural Characteristics of Lignin in Hydrothermal Pretreated Fibers and Manufactured Binderless Boards from Eucalyptus Grandis. *Sustainable Chem. Processes* **2014**, *2*, 9.
(47) Kljun, A.; Benians, T. A.; Goubet, F.; Meulewaeter, F.; Knox, J. P.; Blackburn, R. S. Comparative Analysis of Crystallinity Changes in Cellulose I Polymers Using ATR-FTIR, X-Ray Diffraction, and Carbohydrate-Binding Module Probes. *Biomacromolecules* **2011**, *12*, 4121−4126.
(48) Poletto, M.; Pistor, V.; Santana, R. M. C.; Zattera, A. J. Materials Produced from Plant Biomass: Part II: Evaluation of Crystallinity and Degradation Kinetics of Cellulose. *Mater. Res.* **2012**, *15*, 421−427.
(49) Oh, S. Y.; Yoo, D. I.; Shin, Y.; Seo, G. FTIR Analysis of Cellulose Treated with Sodium Hydroxide and Carbon Dioxide. *Carbohydr. Res.* **2005**, *340*, 417−428.
(50) Park, S.; Baker, J. O.; Himmel, M. E.; Parilla, P. A.; Johnson, D. K. Cellulose Crystallinity Index: Measurement Techniques and Their Impact on Interpreting Cellulase Performance. *Biotechnol. Biofuels* **2010**, *3*, 10.
(51) Saha, P.; Manna, S.; Chowdhury, S. R.; Sen, R.; Roy, D.; Adhikari, B. Enhancement of Tensile Strength of Lignocellulosic Jute Fibers by Alkali-Steam Treatment. *Bioresour. Technol.* **2010**, *101*, 3182−3187.
(52) Segal, L.; Creely, J. J.; Martin, A. E., Jr; Conrad, C. M. An Empirical Method for Estimating the Degree of Crystallinity of Native Cellulose Using the X-Ray Diffractometer. *Text. Res. J.* **1959**, *29*, 786−794.
(53) Aryal, G. M.; Aryal, B.; Kandel, K. P.; Neupane, B. B. Cellulose-Based Micro-Fibrous Materials Imaged with a Home-Built Smartphone Microscope. *Microsc. Res. Tech.* **2021**, *84*, 1794.
(54) Ilyas, R. A.; Sapuan, S. M.; Ishak, M. R.; Zainudin, E. S. Sugar Palm Nanofibrillated Cellulose (Arenga Pinnata (Wurmb.) Merr): Effect of Cycles on Their Yield, Physic-Chemical, Morphological and Thermal Behavior. *Int. J. Biol. Macromol.* **2019**, *123*, 379−388.
(55) Ilyas, R. A.; Sapuan, S. M.; Ishak, M. R. Isolation and Characterization of Nanocrystalline Cellulose from Sugar Palm Fibres (Arenga Pinnata). *Carbohydr. Polym.* **2018**, *181*, 1038−1051.
(56) Ilyas, R. A.; Sapuan, S. M.; Ishak, M. R.; Zainudin, E. S. Effect of Delignification on the Physical, Thermal, Chemical, and Structural Properties of Sugar Palm Fibre. *BioResources* **2017**, *12*, 8734−8754.
(57) Abral, H.; Ariksa, J.; Mahardika, M.; Handayani, D.; Aminah, I.; Sandrawati, N.; Pratama, A. B.; Fajri, N.; Sapuan, S. M.; Ilyas, R. A. Transparent and Antimicrobial Cellulose Film from Ginger Nanofiber. *Food Hydrocolloids* **2020**, *98*, 105266.
(58) Samy, M. M.; Mohamed, M. G.; Mansoure, T. H.; Meng, T. S.; Khan, M. A. R.; Liaw, C.-C.; Kuo, S.-W. Solid State Chemical Transformations through Ring-Opening Polymerization of Ferrocene-Based Conjugated Microporous Polymers in Host−Guest Complexes with Benzoxazine-Linked Cyclodextrin. *J. Taiwan Inst. Chem. Eng.* **2022**, *132*, 104110.
(59) Beckermann, G. W.; Pickering, K. L. Engineering and Evaluation of Hemp Fibre Reinforced Polypropylene Composites: Fibre Treatment and Matrix Modification. *Composites, Part A* **2008**, *39*, 979−988.
(60) Dufresne, A. Cellulose-Based Composites and Nanocomposites. *Monomers, Polymers and Composites from Renewable Resources*; Elsevier, 2008; pp 401−418.

https://doi.org/10.1021/acsomega.2c04398
ACS Omega 2022, 7, 32717−32726